Chapter 9

Global Machinability of Al-Mg-Si Extrusions

V. Songmene, J. Kouam, I. Zaghbani, N. Parson and A. Maltais

Additional information is available at the end of the chapter

http://dx.doi.org/10.5772/54021

1. Introduction

Field performance, mechanical properties and workability usually sustain the development of new alloys. As far as the workability is concerned, most extrusions need not only to meet good extrudability, but also good or acceptable machinability as some machining operations (eg. drilling or finishing machining) are usually required. Unfortunately, alloys with higher strength could have better machinability but lower extrudability; Aluminum alloys with excellent extrudability such as AA1060 or AA1100 (Figure 1) often exhibit low machinability, especially due to the chip formation and the workpiece material adhering to the cutting tool leading to the build-up-edge (BUE), modifying the cutting process, leading to tool breakage or deteriorating the surface finish when this BUE is broken. Al-Si-Mg alloys (6XXX series) usually exhibit good machinability and good extrudability; This is one of the reason why about 90% of most extruded aluminum parts are in 6XXX family. The AA6262 which is recognized for its ease chip breakability (a lot of second phase particles which help initiate fracture) generally leads to good machinability but poor extrudability because of its poor formability. Any new aluminum alloy with excellent machinability, extrudability and mechanical properties will therefore lead to considerable advantage compared to existing alloys.

Farmer (1978) proposed a system (based on extrusion ratio, die angle, billet length-to-diameter ratio and statistical analysis) for evaluating the extrudability of aluminum alloys and illustrated the system using AA2011, AA6061, AA6063 and AA 6262 aluminium alloys in their T0-temper condition. The extrusion ratio and the extrusion pressure were shown to able to allow benchmarking the tested alloys according to their extrudability. The AA6063 showed the best performance, followed by the AA6061 and the AA6262 wheras the AA2011 exhibited the poorest performance amongst the criterion tested. The performance of the tested alloys found by Farmer (1978) is in good agreement with the data presented in Figure 1. Both the extrusion ratio and the extrusion pressure gave a good picture of true stress-true strain behavior of the tested alloys. It is however important to notice that the machinability of the alloys was not evaluated.

According to Saha (2012), the maximum extrusion speed is one of the most significant factors influencing the cost and efficiency of the extrusion process. This speed can therefore be used to measure the extrudability of alloys. He (Saha, 2012) compared the extrudability of the AA2XXX, AA6XXX and that of the AA7XXX based on major allowing elements. AA6XXX containing Mg and Si had better relative extrudability (100), while alloys of the same family but containing Cu was rated at 60%. AA2XXX series with Cu, Mg, Mn as major alloying element were rated 15% and AA7XXX with Zn, Mg, Cu, Cr as major alloying elements were rate 10%. This classification is in good agreement with the data presented in Figure 1.

Chena et al. (2009) investigated the dynamic fracture behavior (Charpy test) of extruded AA6XXX and AA7XXX aluminum alloys: AA6060, AA6082, AA7003 and AA7108, all in T6 condition. As expected, they found that the AA7XXX which have higher strength (yield and ultimate tensile stresses) exhibited higher toughness than the AA6XXX but the fracture strain of the AA7XX was lower compared to that of the AA6XXX alloys as a consequence of higher precipitation of grain boundary found in AA7XXX. It is therefore understandable that the AA7XXX show poor extrudability as depicted in Figure 1.

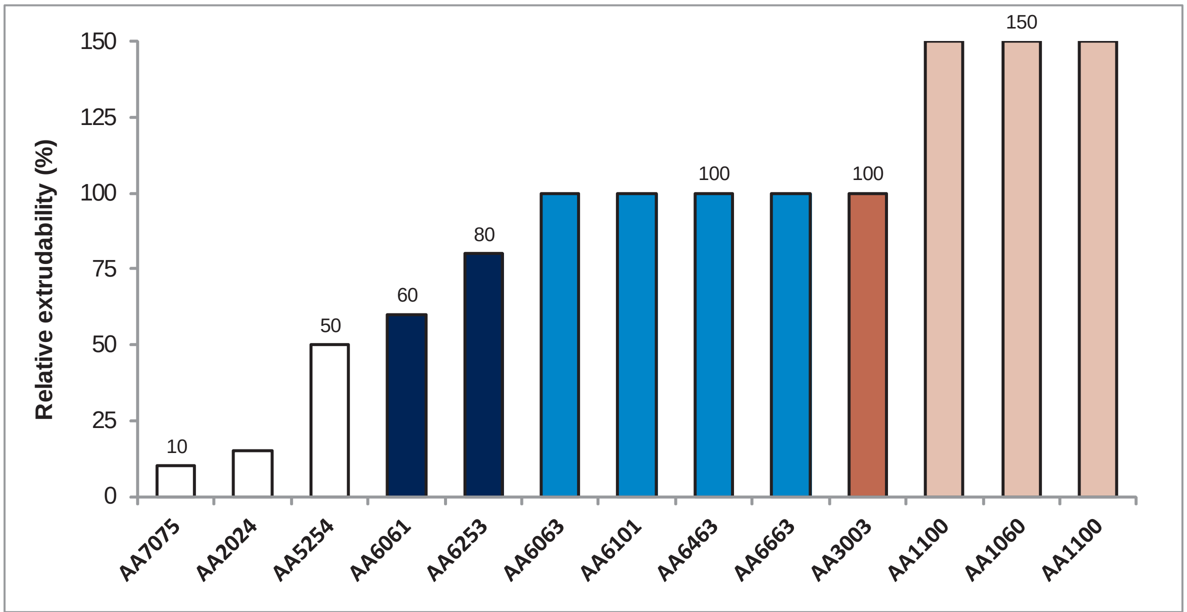

Figure 1. Relative extrudability of some selected aluminum alloys (adapted from Duval, 2012)

Pangborn *et al.* (2012) studied the workability, the mechanical properties of the 6061 and that of the 6005A in T5 and T6 conditions and found that the 6005A has significant advantages over the 6061 in many applications: better toughness, better corrosion resistance, better

http://dx.doi.org/10.5772/54021

quenching sensitivity and better consistency of mechanical properties together with comparable fatigue resistance, machinability rating, formability, weldability, and ease ability to meet minimum mechanical properties with 6061. According to the authors, when initially tried by a customer, <<the 6005A ran at more than twice the extrusion speed, which had resulted in tearing for 6061. The surface finish was excellent and good mechanical properties were obtainer using only air cooling, at the press run-out. No tearing was noted in the 6005A even at highest speed used at the press, indicating the shape could have been pushed even faster>>, Pangborn et al. (2012). After two years period after implementation, the data showed a << net productivity increased over 50 percent in a two year time period>>

Along with the introduction of new material, it has become necessary to characterize the workpiece workability and machinability, Zaghbani et al., (2010). Traditionally, the machinability characterization has been based either on the tool life or on the energy required to shape them, Songmene et al., (1996). In the case of aluminum alloys, the considered criterion for tool life is the tool breakage due to adhesion of the aluminum alloy on the tool as a result of the heat involved in the process or the material ductility. The tool breakage is generally observed for a carbide drill after drilling more than 2000 holes at a depth of around 28.3 mm, Zitoune, (2010). Nouri et al., (2004), while studying the wear mechanism during drilling of aluminium alloys, showed in their study that some of the most important causes of tool wear are the diffusion and adhesion of the material, which could degrade the surface finish. These results were confirmed by List et al., (2005).

In the drilling process, the cutting forces can be a good indicator for a comparison of different alloys under the same machining conditions, Zaghbani and Songmene, (2009). Some authors, such as Shaw (1989), Subramanian et al., (1977), Kouam et al., (2010) and Kouam et al., (2012), have shown that the thrust force increases with the feed rate. In the case of isotropic materials, the cutting forces follow a linear behavior when the feed is varied, Altintas, (2000). For new materials, it is important to verify this behavior. If the behavior is non-linear, this can indicate a high non-homogeneity within the material.

The machinability of an alloy, while not being a standard property, defines its ability to be machined or shaped using a cutting tool (Sandvik, 1994), and can be evaluated using tool wear, tool life, productivity, part quality, cutting forces, or chip form. Songmene et al. (1996) established a procedure for testing the tool life and the machinability of materials and he also defined a global machinability rating taking into account the tool life, the cutting forces, the surface finish and the chip formation. Decreasing the chip size can improve the tool life, the surface finish and lower the energy required for machining. The surface finish is an indicator of the quality of the material following the machining process. One other main difficulty encountered in the machining process is burr formation. Its removal is costly and is considered a non-productive operation. The burr morphology depends on the cutting conditions and the mechanical properties of the workpiece material and on the tool used. Rivero et al., (2006) showed in their work that burr formation could have an influence on power consumption and on the tool temperature. In his work, Gillespie (1973) identified some mechanisms responsible of burr formation: material lateral deformation, chip bending and chip tearing. These mechanisms are of course dependent on workpiece materials, cutting tool geometry and machining strategies. Later, Gillespie et al., (1989) linked burr formation mechanisms with deburring processes and techniques. Deburring is however a non-productive and costly finishing process that must be minimized or avoided. Any material leading to limited burr formation is therefore advantageous.

In general, aluminium alloys generally have good machinability (higher tool life; low cutting forces; higher cutting speeds can be used) but some issues might arise with chip control and management, build-up edge: material adhering on the cutting tool causing poor surface finish and burr formation. Burr removal is costly and is considered as a non-productive although it is a finishing operation. High silicon content aluminum alloys (hyper-eutectic) are usually more abrasive and wear out quicker the cutting tool, especially carbide tooling. Diamond tools should be considered. These tools are expensive but are able to produce a large number of parts before getting dull. The addition or the change in additive elements content can impact the mechanical and the machinability properties, therefore could make a product more or less competitive. In fact, economical and maximum productivity machining conditions (speeds and feeds) depend on the machinability of the workpiece material. Therefore, it is important to develop materials with excellent mechanical and field properties but also with good machinability and it could influence the competitiveness and the acceptability of a given product.

The main objective of this work was to compare the machinability of four Al-Mg-Si aluminum alloys manufactured by Rio Tinto Alcan: AA6262-T6 (37.3 HRA); AA6061-T6HS (39.6 HRA); AA6061-T6 (29.7 HRA) and AA4XXX-T6 (36.6 HRA). The evaluation included tool wear, cutting force, surface finish, chip form and burr height. As the current tendency in most machining shops is to eliminate the lubricant for machining costs reduction purposes and to respect environmental and occupational safety regulations, the dry drilling is used in this work to evaluate machinability.

2. Global machinability model

The machinability can be defined as the relatively ease or difficulty to shape a workpiece material using a cutting tool. Several factor affect the machinability; They include the cutting data and conditions (cutting speed, feed, depth of cut and type of operation- lubricated or not), the tool data (tool material and coating, tool geometry including the rake angle, the lead angle, the clearance angle, the nose radius, the edge preparation); but also the operation (continuous or interrupted) and of course the material. Amongst the workpiece material data affecting the machinability, one can list: the mechanical properties (strength, ductility, toughness, and hardness), thermal conditions, inclusions, work hardening, microstructure, conditions, and chemical composition.

The machinability of a material can be evaluated using one or a combination of the following criteria: cutting tool wear/life, energy required for machining or specific cutting forces, part quality including surface texture, burr formation and chip formation. The global machinability rating developed by Songmene et al., (1996) and refined by Zaghbani et al., (2010) was further improved by adding the sticking tendency and the material ability to form burr. Using specific ratios related to tool life (R_{TL}), sticking tendency (R_{ST}), cutting force (R_{CF}), surface finish R_{SF}, burr height R_{BH} and chip length R_{CL}) the global machinability (GMR) of the tested alloys was assessed:

$$Global \quad Machinability = \lambda_1 \times \cdot Tool\_life_{ratio} + \frac{\lambda_2}{Sticking\_tendency_{ratio}} + \frac{\lambda_3}{Forces_{ratio}} + \frac{\lambda_4}{Burr\_height_{ratio}} + \frac{\lambda_5}{Chip\_length_{ratio}} + \frac{\lambda_6}{Surface\_finish_{ratio}} \tag{1}$$

$$GMR = \lambda_1 \times \cdot R_{TL} + \frac{\lambda_2}{R_{ST}} + \frac{\lambda_3}{R_{CF}} + \frac{\lambda_4}{R_{BH}} + \frac{\lambda_5}{R_{CL}} + \frac{\lambda_6}{R_{SF}} \tag{2}$$

Where λi (i = 1 to 6) are the specific weights: $\lambda_1+\lambda_2+\lambda_3+\lambda_4+\lambda_5+\lambda_6 = 1$; Each ratio (Tool life ratio R_{TL}; sticking tendency ratio R_{ST}; cutting force ratio R_{CF}; surface finish R_{SF}; burr height ratio R_{BH} and chip length ratio R_{CL}) is computed as the ratio of the performance index for the tested material to that of the reference material.

- **Tool life** can be based on a number of holes drilled before the drill is dull. The tool life criteria can be set upon a surface finish value, an increase in cutting forces or on a given drill flank wear value (ie. VB = 0.3 mm).

$$R_{TL} = \frac{Tool\_Life\_M}{Tool\_life\_AA6262} \tag{3}$$

where Tool_life_M is the thrust force of material M and Tool_life_ $_{AA6262}$ is the tool life for the reference AA6262-T6 alloy.

- **Cutting forces:** The ratio of thrust force was used :

$$R_{CF} = \frac{F_z\_M}{F_z\_AA6262} \tag{4}$$

where $F_{z\text{-}M}$ is the thrust force of material M and $F_{z\text{-}AA6262}$ is the thrust force for the reference AA6262-T6 alloy.

- **Material sticking:** One of the issues that may interest a machinist dealing with aluminum alloys is sticking. It is known that some aluminum alloys exhibit a high sticking tendency, which is due mainly to their relatively high thermal conductivity. This causes thermal softening, which leads to the sticking of the work piece material to the tool. During machining, this problem can be observed on different regions of the tool, with the greatest concentration being on the chisel edge where the cutting speed is at its lowest. However, it is difficult to arrive at a conclusion as to which material sticks more than the others based on these images. Normally, the material that sticks the most is the one that will accumulate the highest quantity of metal on the chisel edge. However, as the adhered material can be removed from one hole to another, comparing the accumulated quantity of materials for each alloy is complex. For these reasons, a new criterion for sticking is proposed. This criterion is based on a variation of the axial cutting force. It is known that a new tool has no adhered material on it, and so the cutting force generated using such a tool can be considered as a reference force. As material stick to a new tool, its geometry changes. If a second hole is drilled with the same tool (now with adhered material on its chisel edge) the "new tool geometry" will cause a variation of the cutting force, with this variation being proportional to the adhered material. This criterion which characterizes the sticking tendency (ST) can be defined as the variation of the cutting forces knowing that no flank wear will occur when drilling one hole on aluminum :

$$Sticking\_Criterion = ST = \frac{\Delta F}{F} = 1 - \frac{Max\_F_z\_hole\_1}{Max\_F_z\_hole\_2} \tag{5}$$

The higher is the value of ST (Criterion of sticking) the higher is the tendency of the material to adhere to the tool. Using the proposed sticking criterion, ST, it is possible to rationally compare each alloy tested to the reference AA6262-T6 alloy in terms of sticking. From the sticking tendency of each alloy (Eq. 5), the sticking tendency ratio R_{ST} was defined as:

$$R_{ST} = \frac{ST\_M}{ST\_AA6262} \tag{6}$$

- **Burr formation:** Burrs produced during machining affects the quality of part, especially for precision component, and can easily jeopardize the assembly and the functionality and the life of the components and machines. They cause misfits in precision assembly, blockage in internal ducts during operation (when detached) and early failure of the component, Olvera and Barrow (1995). Deburring and edge finishing in aerospace industry can easily represent 30% of part cost (Gillespie, 1973), or 10-12 % of total machining time. Deburring, like inspection, is a non-productive operation and, as such, should be eliminated or minimized to the greatest extent possible, Dornfeld (2004). Burr control is necessary to improve workers safety, reduce manufacturing and assembly costs and to improve the productivity.

The burr form and height are dependent on the material properties and cutting conditions. A material generating fewer burrs is therefore more interesting than a one generating more. The ability of a given material to generate burr can therefore be a measure of its machinability. To do so, the burr type or the burr size could be used to compare the machinability. Let's R_{BH} be the ratio of the burr size for a tested material compared to the AA6262-T6 reference material.

$$R_{BH} = \frac{BH\_M}{BH\_AA6262} \tag{7}$$

http://dx.doi.org/10.5772/54021

where BH_{-M} is the burr height of material M and $BH_{-AA6262}$ the burr height of the AA6262-T6 alloy.

- **Chip formation:** The success of a machining operation can also be determined by the chip formation which is strongly associated with the properties of the workpiece material and the cutting conditions. Short and discontinuous chips are usually preferred for chip management purpose and also because of their beneficial indirect effects on tool life, surface finish, cutting forces/energies and on metallic particle emission (Songmene et al., 2011). The chip length ratio (R_{CL}) was computed as follow:

$$R_{CL} = \frac{CL\_M}{CL\_AA6262} \tag{8}$$

where CL_{-M} is the measured chip length of material M and $CL_{-AA6262}$ that of the reference AA6262-T6 alloy.

- **Surface finish:** For the surface finish ratio, the arithmetic average roughness (Ra) was used.

$$R_{SF} = \frac{Ra\_M}{Ra\_AA6262} \tag{9}$$

For the evaluation of the global machininability of the Al-Mg-Si alloys (Equation 2), the weights (coefficients of Equation 2) were varied according to potential interest that could be encountered in metal working industries.

3. Al-Mg-Si alloys: Microstructures and manufacturing conditions

The tested materials were manufactured by Rio Tinto Alcan: AA6262-T6 (37.3 HRA); AA6061-T6HS (39.6 HRA); AA6061-T6 (29.7 HRA) and AA4XXX-T6 (36.6 HRA). All four alloys were DC cast and subjected to commercial homogenization cycles. The AA6061 was a typical commercial variant of AA6061 suited for high speed extrusion into thinner wall shapes. The AA6061 High Strength (AA6061HS) contained higher levels of the major alloy addition to promote increased age hardening response. The AA6262 and AA4XXX compositions were based on AA6061 but contained additions of 0.5 wt% Pb -0.4 wt% Bi and 8% Si respectively. The AA6061 variants were DC cast directly as 101mm diameter billet whereas the AA4XXX and AA6262 were commercially cast as 300mm dia. The billets were extruded on the 780 tonne, 101mm dia. RTA extrusion press into a 3 x 41mm strip with an extrusion ratio of 70/1. The section was water quenched and aged for 8hrs/170°C to give the T6 temper. Extrusion exit temperatures were in excess of 510°C to promote good press solutionising. Typical extruded microstructures and associated second phase particle distributions are shown in Figure 2.

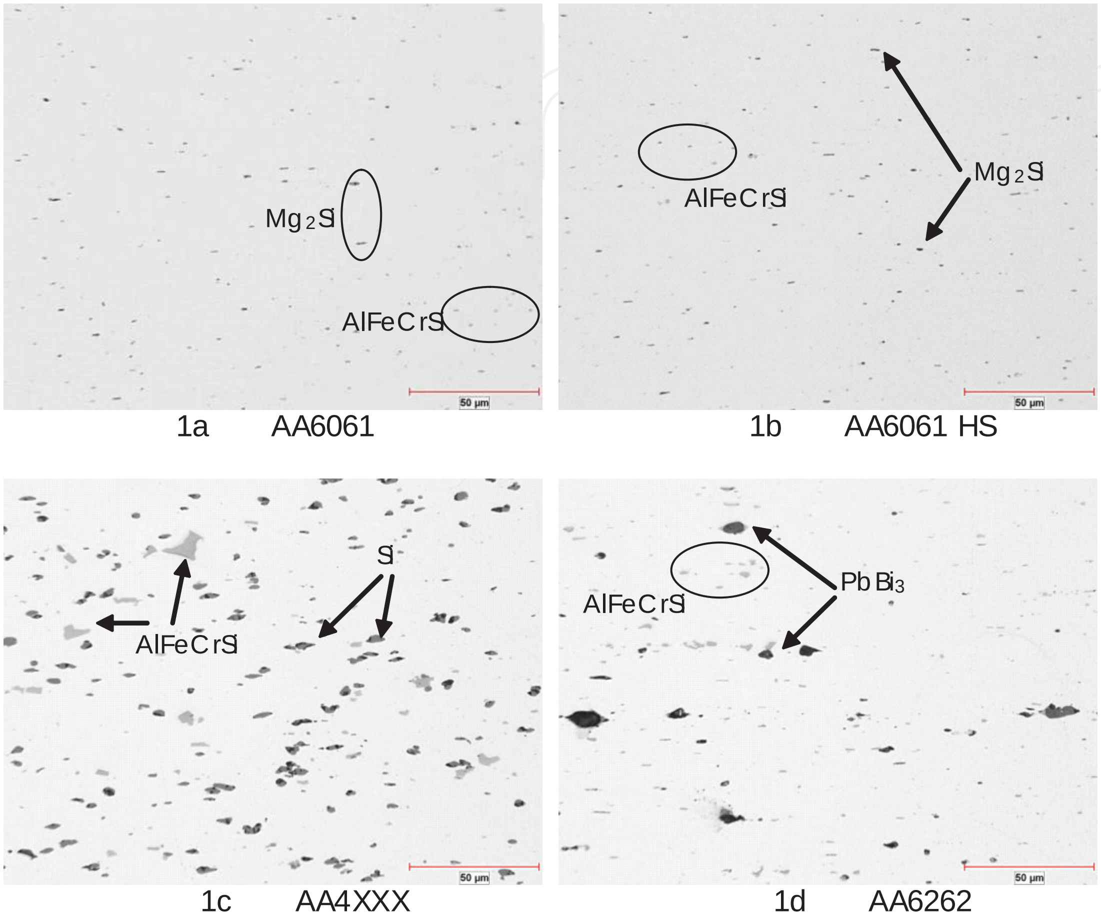

Figure 2. Extruded microstructures (longitudinal, as polished)

The AA6061 variants contained fine Al-Fe-Si intermetallics (grey) and a small volume fraction of undissolved Mg_2Si which is normal for AA6061. As expected, the AA4XXX material with 8% Si contained a much higher volume fraction of second phase consisting of Si particles (dark grey) ~ 5 microns in size and Al-Fe-Si (light grey). The latter was coarser than in the AA6061 variants due to the increased ingot diameter. The main feature of the microstructure in the AA6262 was the globular low melting point $BiPb_3$ particles ~ 2-12 microns in size. The extruded grain structures are shown in Figure 3. The AA6061, AA4XXX and AA6262 extrusions were all fully recrystallised but with varying grain size. The AA6061 HS exhibited a mixed fibrous/partially recrystallised structure.

http://dx.doi.org/10.5772/54021

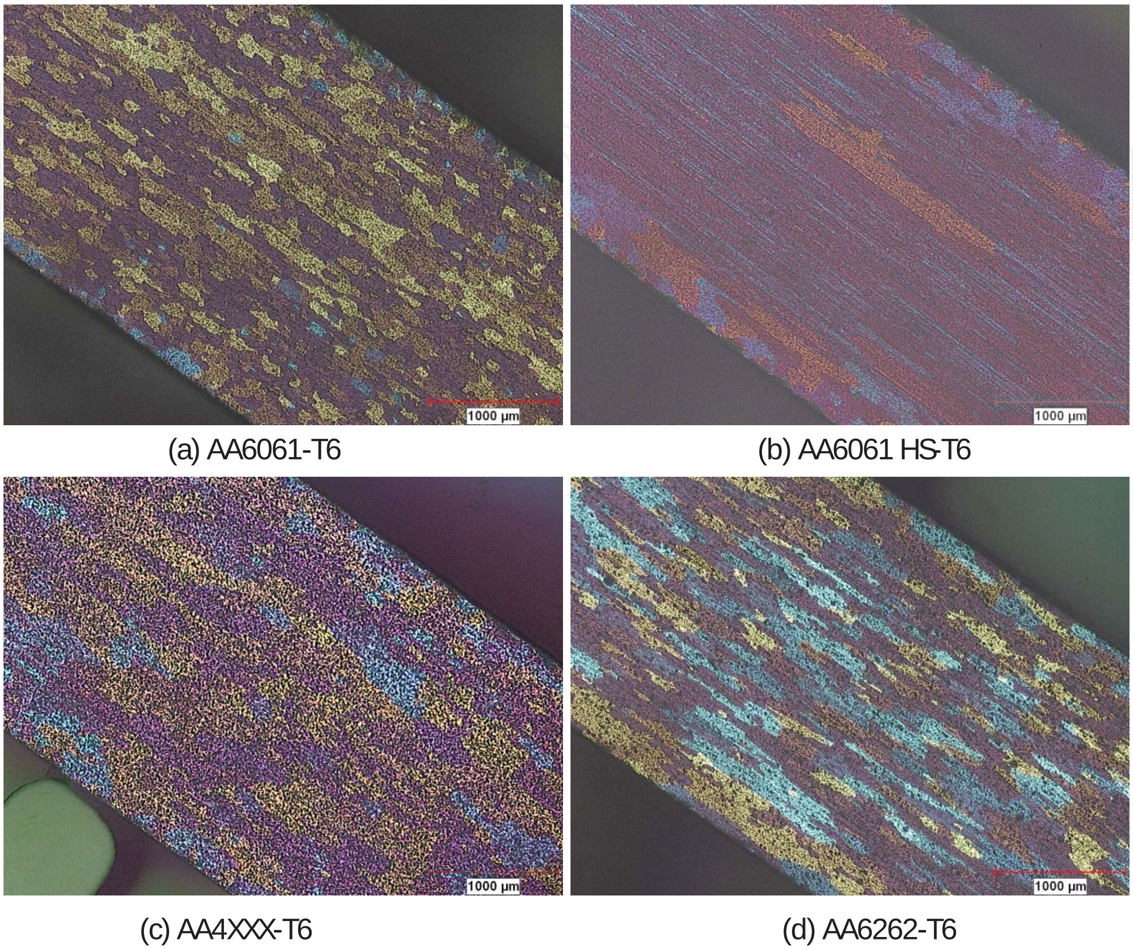

Figure 3. Extruded Grain Structures (Barkers Reagent)

The tensile properties are summarized in Figure 4, with the alloys ranked in terms of increasing strength. The yield strength matches the hardness data presented in section 4 except for the AA4XXX-T6 which gave the lowest yield strength but the second highest hardness. This discrepancy is probably due to the high volume fraction of silicon particles in the microstructure.

All alloys satisfied AA6061-T6 minimum properties but the overall range of yield strength was ~ 60MPa. Toughness was measured using the Kahn Tear test and results are presented in Figure 5. The AA6061-T6 variants exhibited the highest toughness. Normally toughness is expected to fall with increasing yield strength but the AA4XXX-T6 and AA6262-T6 materials did not follow this trend and gave lower toughness for the same or lower yield strength, probably due to the increased volume fraction of coarse second phase particles.

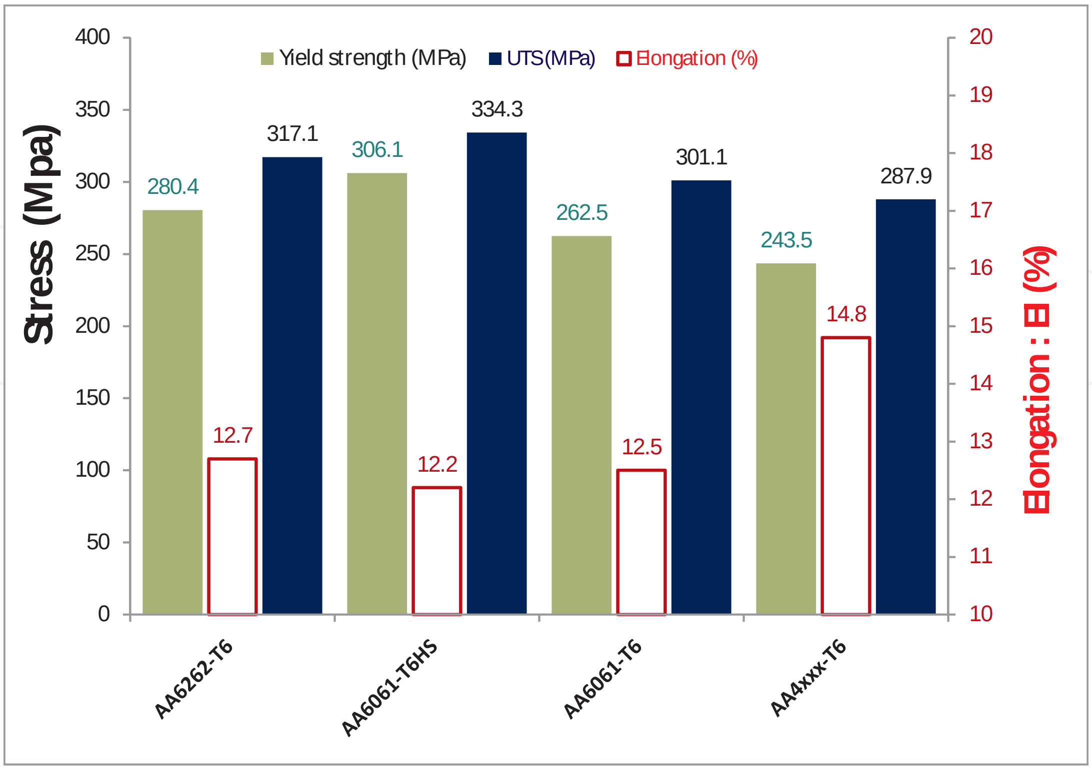

Figure 4. Tensile properties of the tested materials

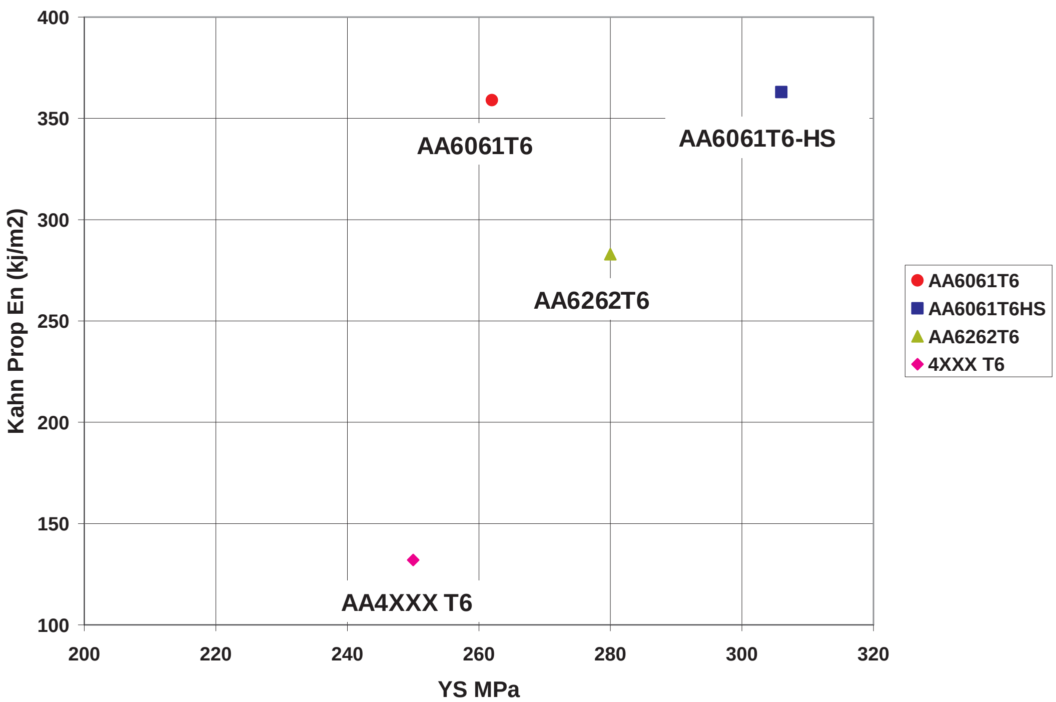

Figure 5. Toughness properties of the tested materials

http://dx.doi.org/10.5772/54021

4. Experimental procedure

The procedure used in this study for machinability testing consisted of drilling parts and recording the following machinability indicators:

- The tool life during drilling operations;
- The surface finish of drilled holes;
- The peak and average values of the cutting force when drilling holes;
- The exit burr height of drilled holes;
- Chip form and chip formation mechanism during drilling and milling.

All these information are necessary for better machinability characterization as presented in section 2- Global machinability model.

The machine-tool and instruments used in the present study are displayed in Figure 6. They consisted of:

- A vertical CNC milling machine-tool (Mazak NEXUS 410 A: 10,000 rpm, 20 hp) which was used to drill the samples or to perform milling operations necessary for chip formation study; Such an industrial scale machine-tool was necessary to reach speeds and conditions currently used in industries. The workpieces were mounted on a 3-axis table dynamometer (Kistler 9255B) to allow the measurement of axial cutting forces during the drilling operations.
- A surface measuring instrument (Mitutoyo SUFTEST SV 600) was used to measure the hole surface finish after the tests;
- An optical microscope (tool maker microscope) equipped with a digital camera, Clemex captive, was used for tool wear inspection and measurement;
- A scanning electron microscope (Hitachi) was used for tool wear mechanisms and patterns studies and for chip form analysis;
- A high speed camera (120 000 fps) was used to study the chip formation during the milling process conducted using the machine-tool presented above.

The following drilling parameters and conditions were used:

- Tool :uncoated high speed steel (HSS); diameter: 9.525 mm (3/8 inch); helix angle:30°; Taper angle: 110°
- Feed per tooth: 0.1016 mm/rev to 0.2286 mm/rev
- Cutting speeds: 45 m/min to 274 m/min
- Each test was repeated 10 times except for the tool wear test which was not repeated because of the large number of holes required (about 1500 holes).
- Lubrication: none

The microstructures, the composition, the temper designations, the manufacturing conditions and the mechanical properties of the alloys tested were described in section 3: These alloys can be summarized as:

- AA6262-T6 (37.3 HRA)
- AA6061-T6HS (39.6 HRA)
- AA6061-T6 (29.7 HRA)
- AA4XXX-T6 (36.6 HRA)

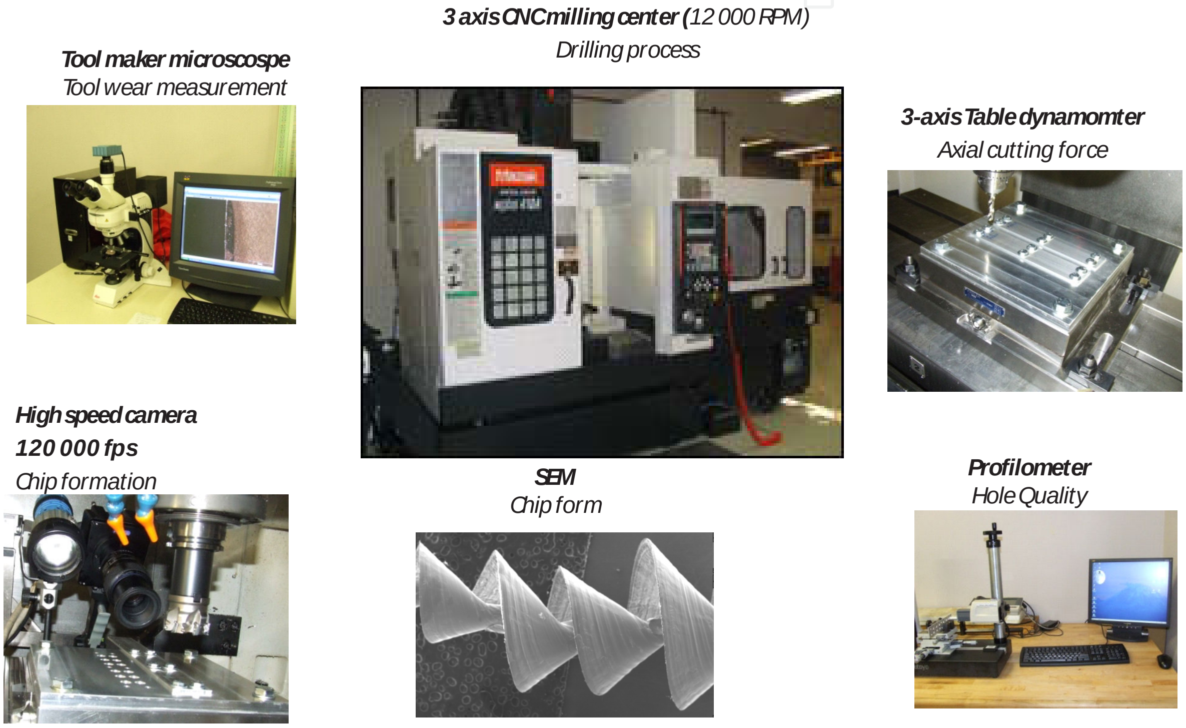

Figure 6. Images of equipment used

5. Results and discussions

5.1. Cutting forces

Figure 7 presents a typical axial force-time data for the four alloys acquired at a sampling frequency of 48 kHz. This high sampling frequency permitted accurate tracking of cutting force variations at the tool tip contact until the retreat of the tool. The similarity of the cutting force profiles for different alloys allows a reasonable comparison of their amplitude. A typical drilling force profile presents different process stages: drill engagement (P1-P2); cutting (P2-P3); deformation of the uncut material leading to burr formation (P4) and drill exit (P4-P5). Following these stages, the drilling process performance can be assessed. Generally, the average or the peak cutting force evaluated when the drill is in full action (between points P2 and P3) can be used to compare different alloys in terms of amplitude of the axial cutting forces. This force can then be plotted against the materials, the workpiece conditions or the cutting parameters.

The variation of the cutting force as a function of feed rate was established in terms of maximum force, and the results are presented in Figure 8. For all the tested alloys, the cutting force followed a linear trend with feed rate. This observation confirms the work by other authors, such as Shaw (1989), Subramanian et al. (1977), Songmene et al. (2011) and Kouam et al. (2012). The linearity was confirmed by correlation coefficients higher than 99%.

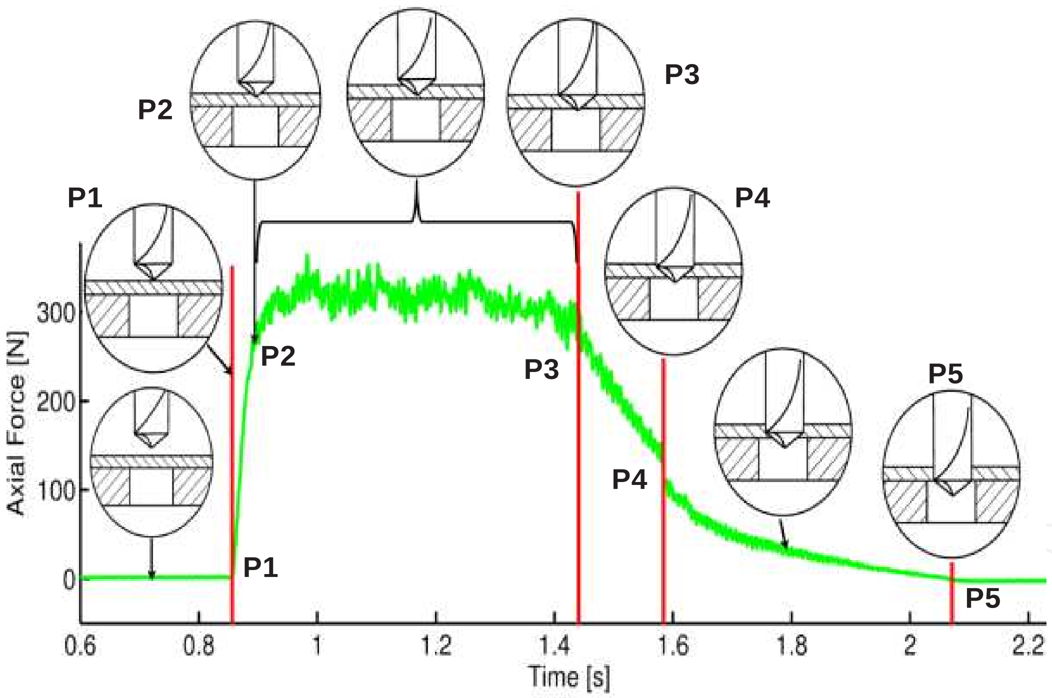

Figure 7. Typical axial force profile during drilling of AA6262-T6

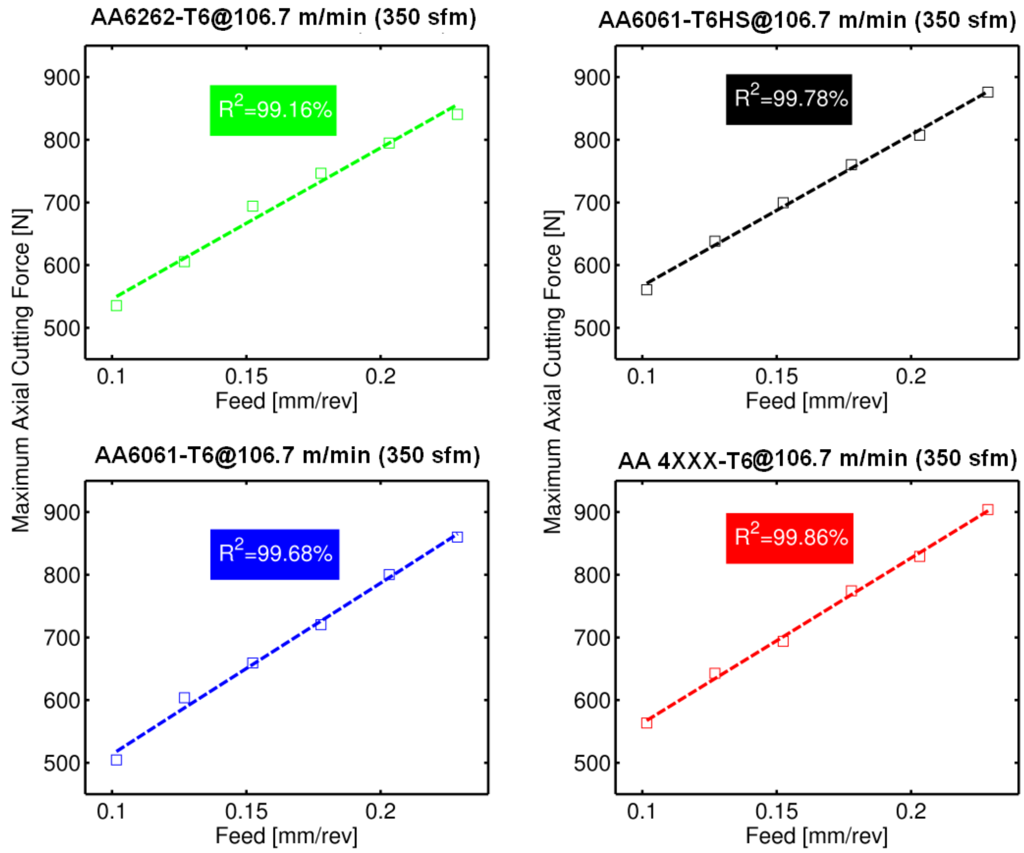

Figure 8. Variation of the maximum axial force of different alloys at different feed rates

Taking into account the decomposition of the axial force into shearing and indentation components (as suggested by Kouam et al. 2010 and 2012), the results in Figure 8 allow the maximum cutting force to be written as a function of the feed and tool radius as follow:

$$F_z = K_d(f \cdot r) + F_{indentation} \tag{10}$$

where : F_z (N) is the maximum cutting force for a given alloy.

- K_d (N/mm²) is mathematically the slope of the line, and physically, represents the resistance of the material to deformation or extrusion during the drilling process.
- r (mm) the tool radius and f (mm/rev) the feed rate;
- $F_{indentation}$ is mathematically the coordinate at the origin, and physically, represents the indentation effect ($f \approx 0$) which describes the resistance of the material to penetration. The indentation force is proportional to the material hardness as shown in Figure 9a.

The plot in Figure 9b shows that both the resistance to deformation (K_d) and the indentation force are needed to better estimate the axial force as no correlation appears between the indentation force and the resistance K_d. The 6061-T6 alloy presented the higher K_d-value, meaning that for a given feed rate, the increase in cutting axial force for this alloy is higher and compensate for the low indentation force.

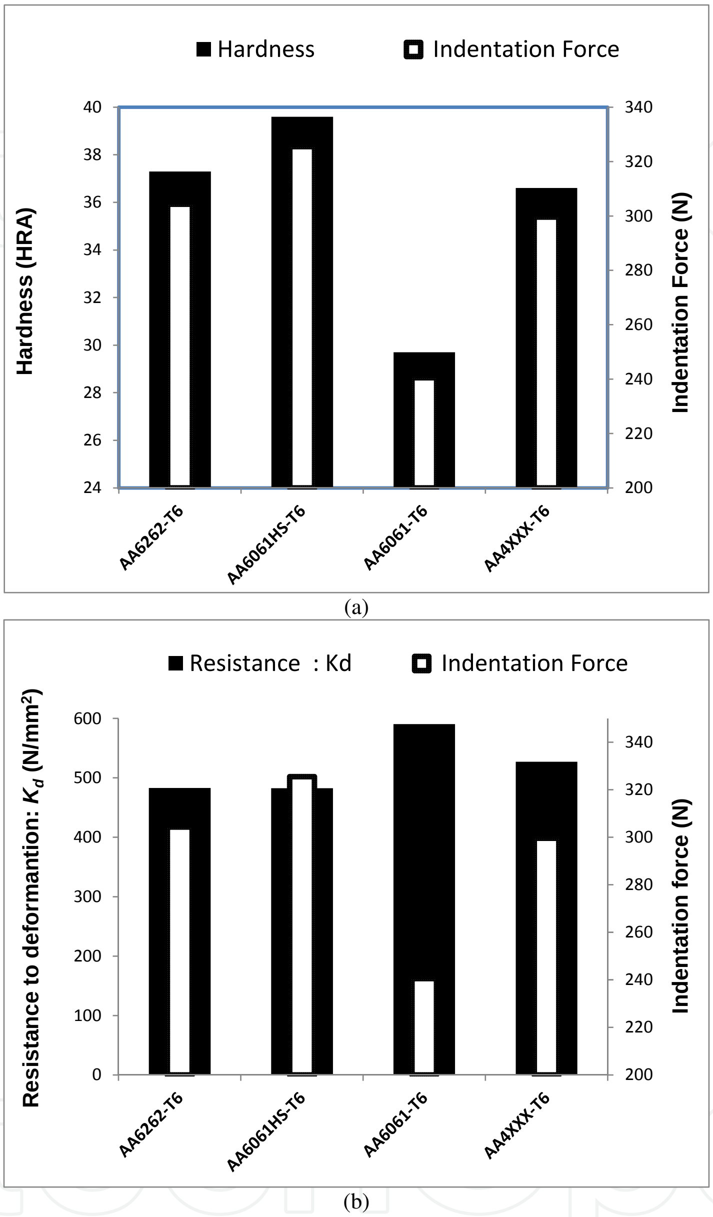

Figure 9. Comparison of components of maximum axial forces (Eq. 10): a) Correlation between the indentation force and hardness; b) comparison between indentation force and the resistance to deformation

Statistical analysis of the cutting forces revealed that there is a significant difference in the behaviour of the four tested alloys in terms of force (average force and maximum peak force). The AA6262-T6 alloy required the lowest force while the AA4XXX-T6 required the highest force (Figure 10). This can be related to the presence of second phases within the alloys (See Figure 2). The 6061-T6 and the 6061-T6HS alloys which had comparable ductility (Figure 4) and toughness (Figure 5) showed comparable cutting force.

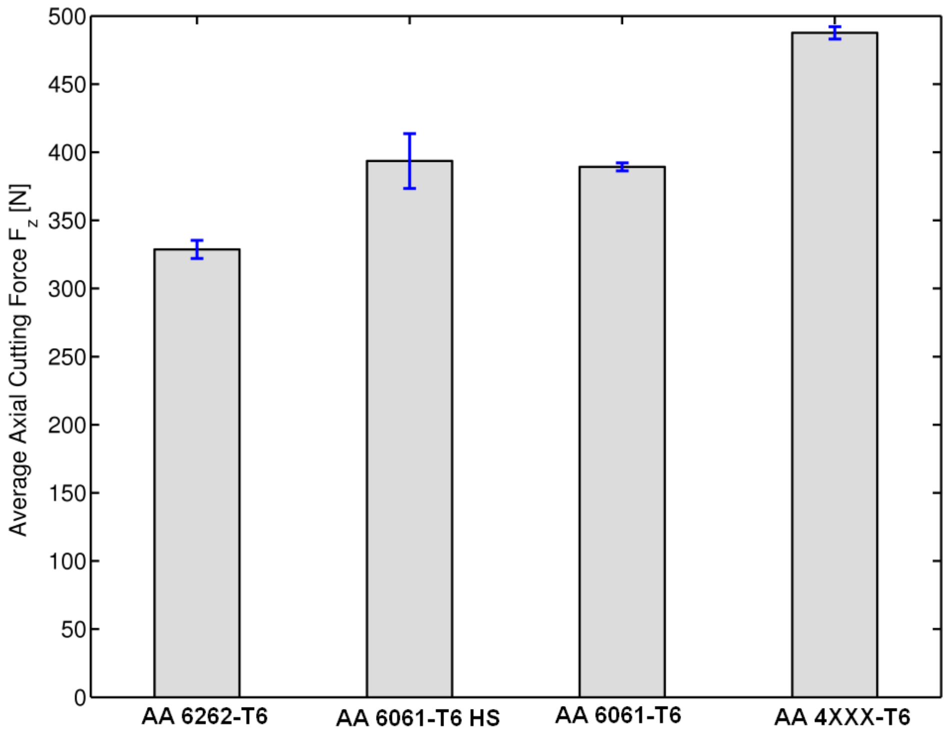

Figure 10. Average axial cutting forces comparison

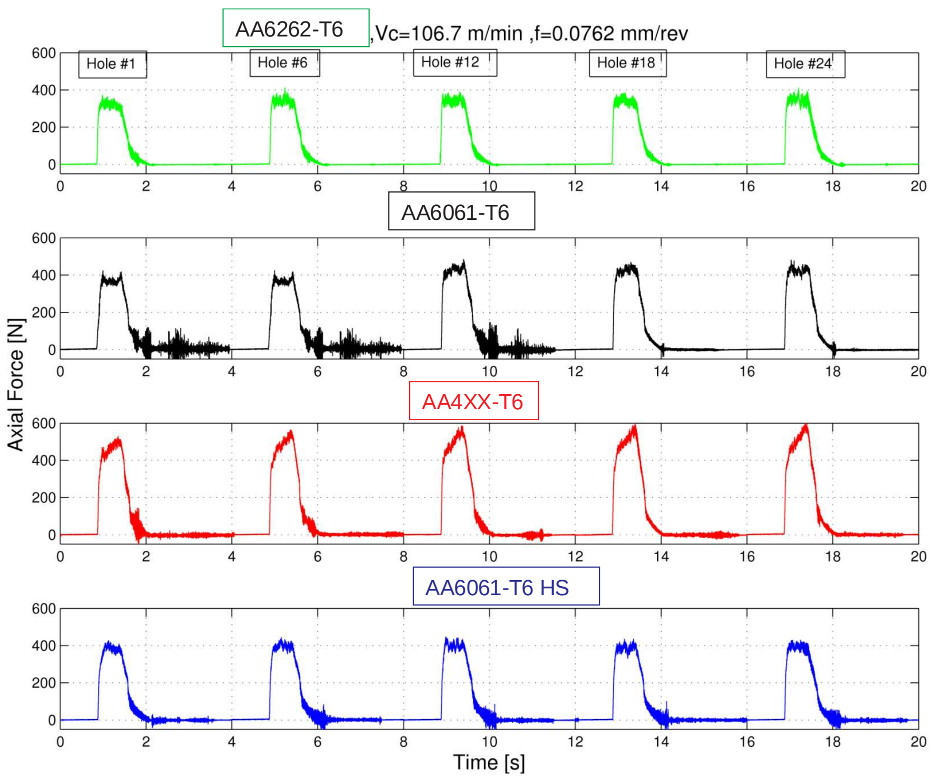

Figure 11. Effect of possible tool wear or material adhesion on cutting force profiles

The force profiles were compared to check for possible tool deterioration (wear, material adhesion, etc.) that could affect the cutting forces, Figure 11. The force profiles recorded for each material repeated themselves well for the first 24 holes drilled, except for the AA6061-T6 for which the first, the sixth and the hole number twelve were different. This difference can be attributed to a possible adhesion of the material on the cutting tool, which might have modified its geometry and led to a different burr formation when the drill exited. Based on the figure 11, it can be reinforced that for the first 24 holes, the cutting did not experienced a wear susceptible of altering the cutting forces.

5.2. Tool wear and tool life

Figure 12 presents SEM images of the cutting lips after drilling many holes. It was observed that the separate drills used to machine the four alloys exhibited a normal tool life under the test conditions used and no premature tool wear or breakage occurred during the drilling tests. The criterion for tool life that is generally considered for aluminum alloys is tool breakage. Each tool was examined by SEM after drilling a given number of holes (432, 856 and 1439 holes), to detect any significant wear on the cutting lips or on the chisel edge.

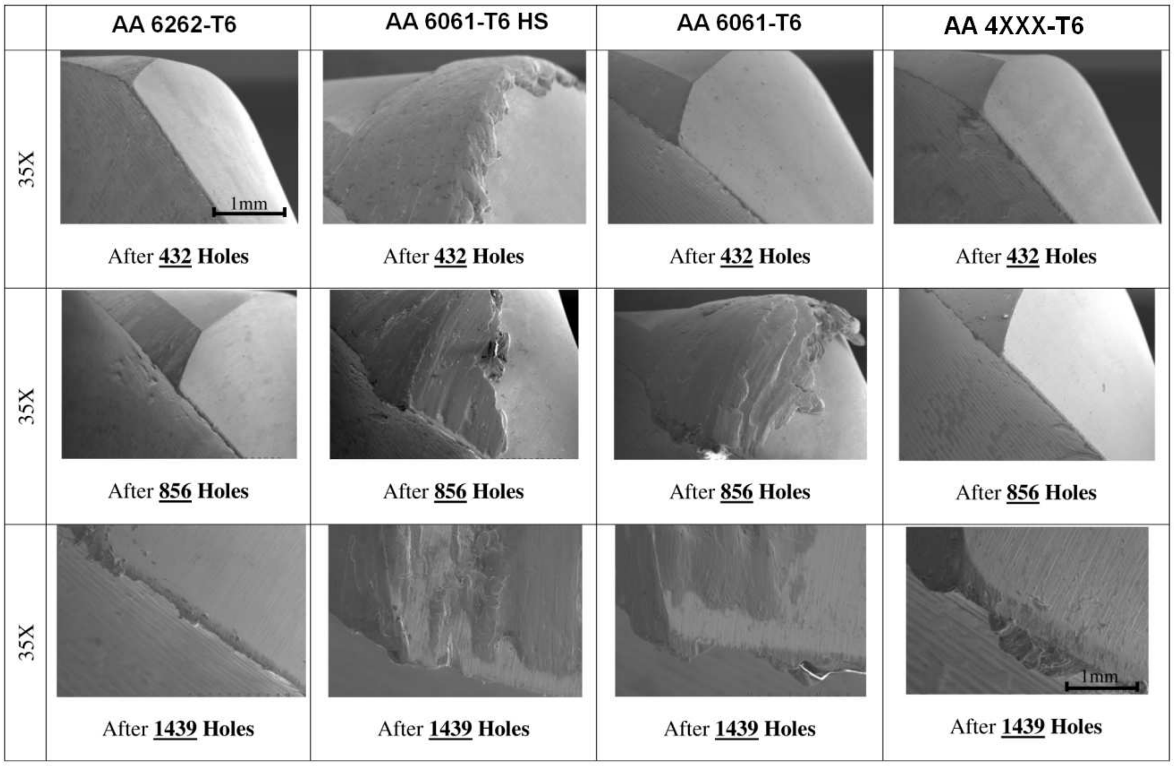

Figure 12. SEM images of the chisel edge after drilling many holes (magnification 35X)

When the number of holes was approximately doubled (856 holes), the cutting lips again did not show any significant wear, as can be seen in the second row of Figure 13. However, when the number of holes reached 1439, the AA6061-T6 HS alloy (second column-third line) began to exhibit significant wear. The arrow added to the graph points to the region of cutting lip wear. The latter was observed at higher magnification (200 X). The SEM images of the cutting lip of the drill used for machining the AA6061-T6HS are presented in Figure 13.

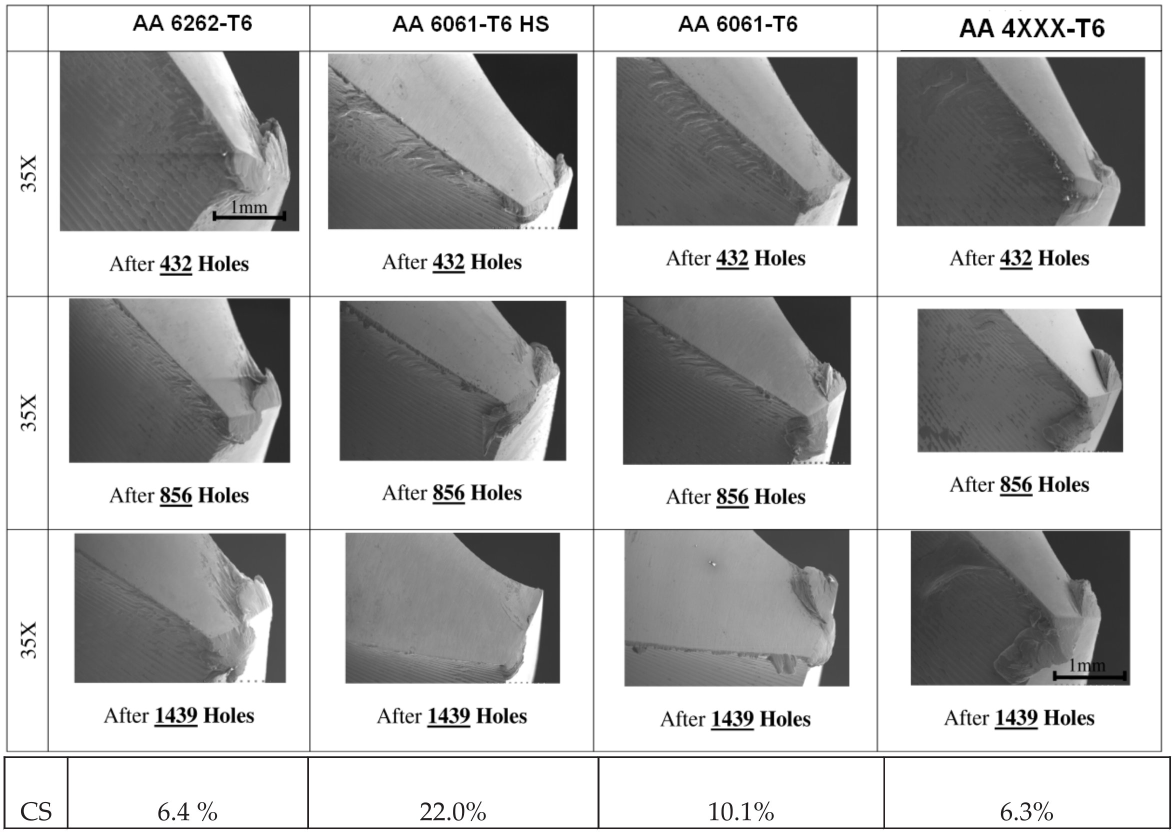

Figure 13. Validation of the sticking criterion (Cs, Eq. 5) with microscopic observations

In general, the four tested aluminum alloys exhibited normal tool life:

- No tool breakage failure was observed for the 1439 drilled holes per alloy,
- No significant tool wear was observed for 1286 drilled holes,
- The aluminum alloy that caused the highest tool wear was the AA6061-T6HS; This can be explained by high mechanical resistance.

It can be considered that the two alloys AA6061-T6 and AA4XXX-T6 have the same tool life as the reference alloy AA6262-T6. While a tool life index (Equation 3) of 94% can be assigned to the AA6061-T6HS. The number of drilled holes with no significant wear was 1286 holes; at 1439 holes there was a significant wear. It can be assumed that the tool wear appeared between 1286 and 1439 holes around 1362 holes.

The sticking tendency of the alloys was evaluated using Equation 5 and the cutting forces profiles. The sticking tendency was confirmed with SEM observations of the drill tips (Figures 12 and 13) and good correlations were found between the sticking tendency and the tool life (Figure 14). Materials with low sticking tendency led to higher tool life (case of the AA6262-T6, AA6061-T6HS and AA4XXX-T6), while the one with high sticking tendency led to lower tool life, Figure 14. When the workpiece material adheres to the cutting tool tip, it modifies the tool geometry, thus increasing the forces required to cut the metal. The surface finish of the machined part is also deteriorated in presence of a built-up-edge; the modification of the tool geometry changes the shearing direction and when the BUE is evacuated, it move to the tool-workpiece interface and contribute to the 3-body wear.

The higher is the value of CS (Criterion of sticking) the higher is the tendency of the material to adhere to the tool. Using this CS, it was possible to rationally compare the four alloys in terms of sticking as shown in Figure 14.

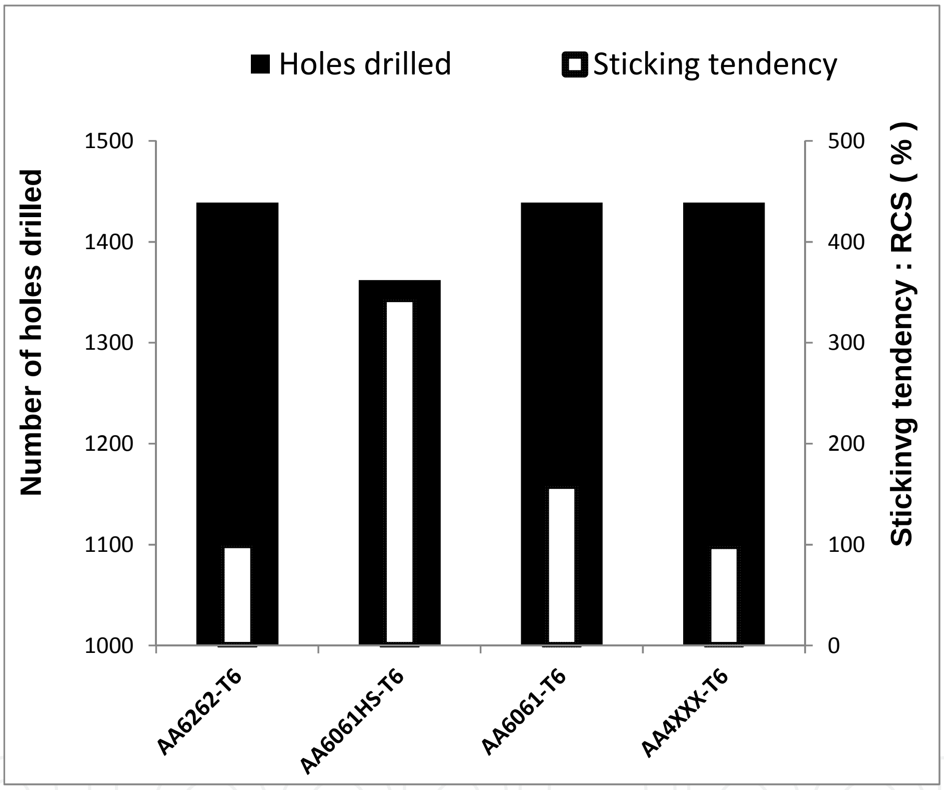

Figure 14. Tool performance and sticking tendency comparison

5.3. Surface quality

Figure 15 presents the average roughness (Ra) and the quadratic roughness (Rq) of holes produced when drilling the different materials. A statistical analysis confirmed that the roughnesses of the four tested alloys are statistically different. The best surface roughness (Ra and Rq) is obtained for the AA6061-T6HS which also exhibited the highest yield strength while the higher values of Ra and Rq were obtained for the AA6262-T6 material. The performance of the AA6262-T6 could be related to sticking of workpiece material onto the cutting edge of the tool (see Figure 12, sticking tendency), forming the build-up-edge

(BUE). It is known that the BUE is usually responsible for the deterioration of the machined part surface finish. However, the recorded values of surface roughness for all the four tested alloys are within acceptable ranges. For a drilling operation, a value between 6.3μm and 1.6μm is considered acceptable for general applications. For more demanding applications of Ra value between 1.6μm and 0.8μm is desirable. For each of the four materials, the ratios of Rq to Ra values were between the ASME recommended brackets.

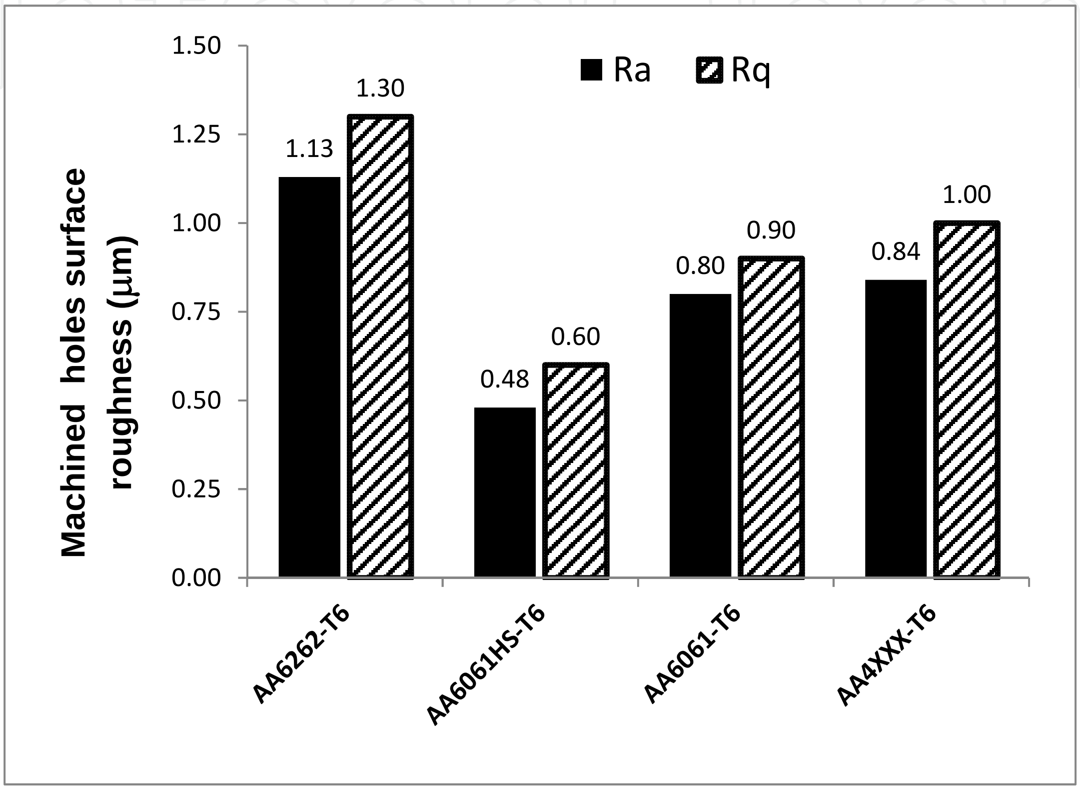

Figure 15. Arithmetic average roughness (Ra) and quadratic roughness (Rq) of holes obtained on different materials

5.4. Burr formation

One other main difficulty encountered during machining of ductile materials is burr formation. Its removal is costly and is considered a non-productive operation. The burr morphology depends on the cutting conditions and the mechanical properties of the workpiece material and on the tool used, Hashimura et al 1999); Rivero et al., (2006) showed that burr formation could have an influence on power consumption and on the tool temperature. Gillespie et al., (1989) linked burr formation mechanisms with deburring processes and techniques.

Burr removal is a non-value added process (Aurich et al. 2009) and might represent as much as 30 percent of the cost of finished parts (Gillespie, 1999). Niknam and Songmene (2012), while modeling and studying the burr formation during milling of AA6061-T6 and AA2024-T321 found that the burr thickness, which control the deburring difficulties and the deburring cycle time, is highly sensitive to material mechanical properties such as yield strength and to the cutting force. As deburring is non-productive and costly finishing process, it should be minimized or avoided. Any material leading to limited burr formation is therefore advantageous.

For assembly purposes, it is important to have holes which are burr-free. For general applications, the hole must be burr-free at a magnification of 5X, while for more critical applications, the magnification can go up to 30 X. The burr form and height are dependent on the material properties and cutting conditions. Images showing typical exit hole appearance are presented in Figure 16 as a function of feed rate. The worst case for burr was obtained for the AA4XXX-T6 (Figure 16) alloy which is the most ductile one. The burr observed was a transient burr type. The other alloys exhibited a uniform burr (type I) or crown burr (type II), Costa (2009):

- The AA6262-T6 and AA6061-T6HS alloys produced only uniform burrs (type II).
- The AA4XXX-T6 and AA6061-T6 alloys produced both uniform burrs (Type II) and transient or crown burrs (type I). The latter are generally difficult to remove.
- The AA4XXX-T6 was problematic in terms of exit burr height.

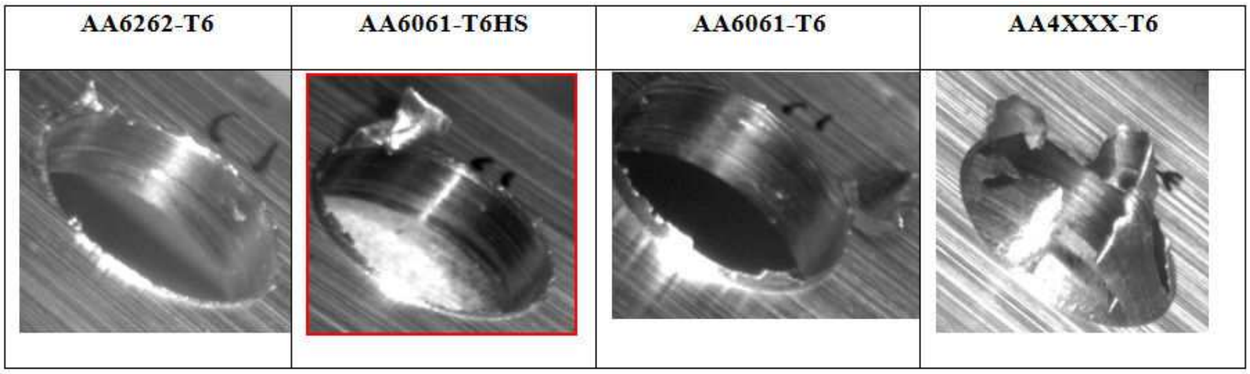

Figure 16. Optical microscopy images of exit burrs observed on drilled holes as a function of feed rate (cutting speed: 45.7 m/min; Feed rate: 0.0508 mm/rev)

In general, the burr form and height was found to be dependent on feed rate, exception of the AA 4XXX-T6 alloy. The lower the feed rate, the higher the burr height obtained, Figure 17. The AA4XXX-T6 produced most of the times high size burrs and only in very limited cases, the burr size was comparable to others alloys tested. At lower speeds, the burr size observed was higher compared the one obtained at high cutting speed; this denotes a possible interaction of the feed rate and the cutting speed on burr formation.

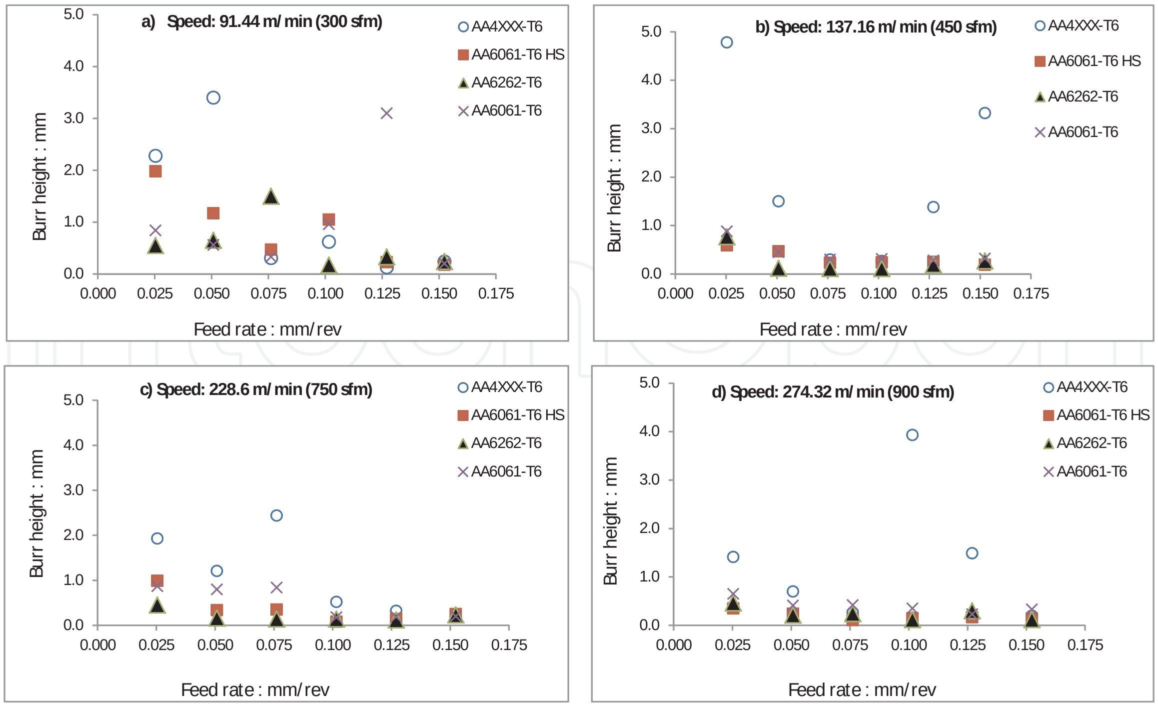

Figure 17. Burr height progression as a function of feed rate, cutting speed and workpiece materials

5.5. Chip formation

The success of an alloy depends also on the chip obtainable during machining of the alloy. A bad chip formation can shorten the tool life, slow down the production, deteriorate the machined part surface finish, increase the machining costs and increase the emission of metallic particles. The AA6262-T6 for example is often preferred for its ability to deliver short and broken chips. Figure 18 displays samples of the chips collected during the drilling of the tested alloys. Under the used cutting conditions, the four tested materials all generated long and continuous chips, but some longer than others (Figure 20).

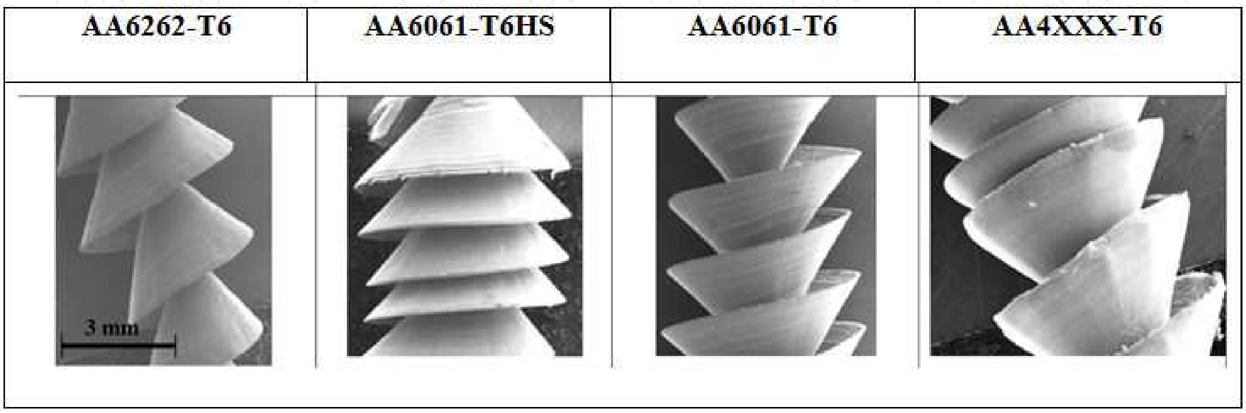

Figure 18. SEM images of the drilled chips (magnification 12 X)

However, during a milling test, a difference was found for example in chip formation for the AA6262-T6 and the AA6061-T6 (Figure 19). The chip formation was recorded using a high speed camera (4 000 fps). In Figure 19, the milling tool progresses for a1 to a3 for the AA6061-T6 and from b1 to b3 for the AA6262-T6. The following observations were made:

- In milling, the chips collected are continuous (Figure 19) and not conical helical as it has been seen in the case of drilling. In figure 19, it can be observed that the produced chips are longer and have more tendencies to adhere to the rake face of the tool. Which may confirm the AA6061 alloy is more adhering than the AA6262, and consequently addition causing more tool wear.
- The chip produced when machining the AA6262-T6 reference material is more curved, leading to high possibility of chip breaking when it comes into contact with workpiece. The difference of chip forms for the four alloys may be explained by the mechanical and thermal properties of each alloy.

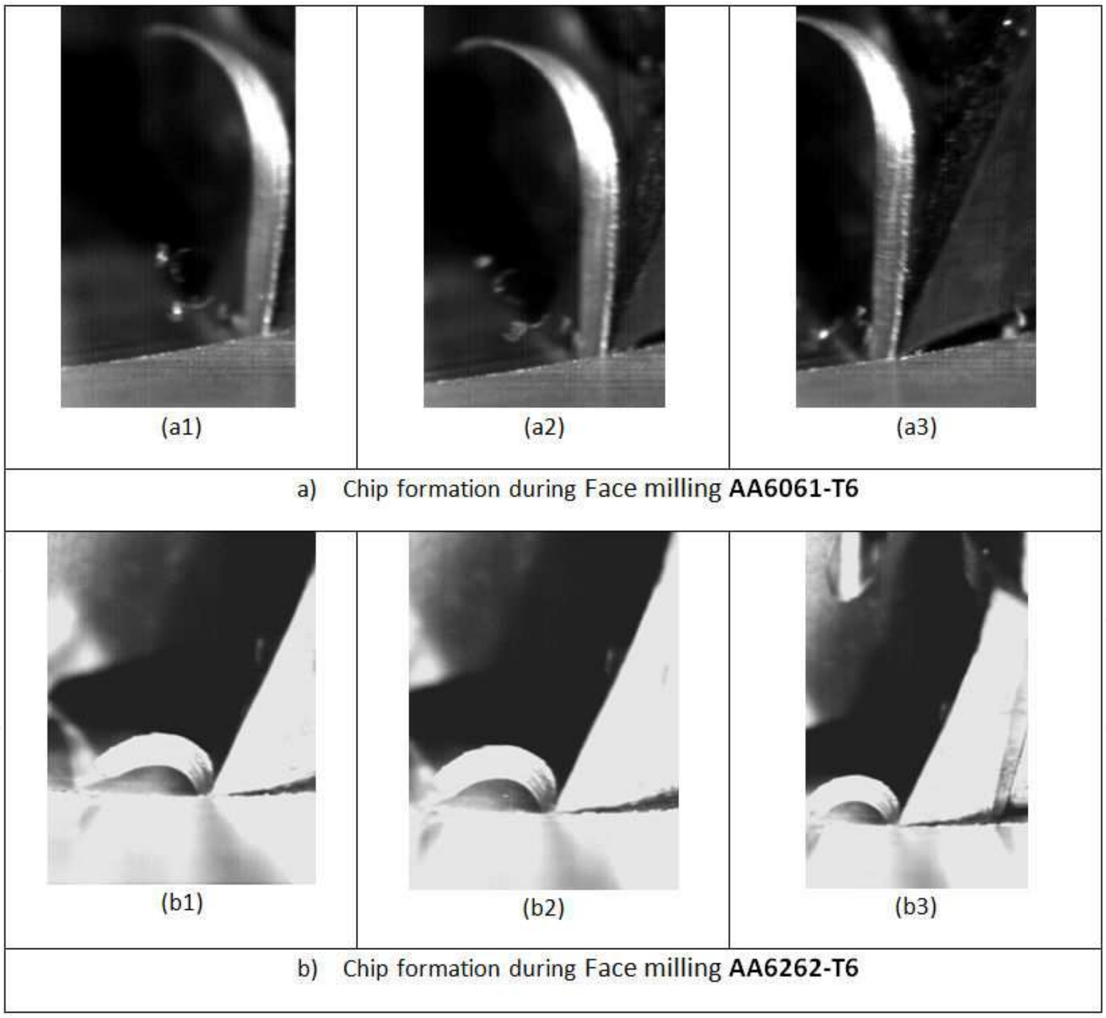

Figure 19. Chip formation during Face milling: feed=0.03 mm/tooth, speed= 191.5 m/min, DOC=1mm; High speed Camera image (4000 fps).

Figure 20 displays the effects of the feed rate and cutting speeds on drilling chip length for each the material tested. It can be observed that the three alloys, AA6262-T6, AA4XXX-T6 and AA6061-T6, behaved similarly in terms of chip length characteristics, which decreased with increased cutting speed and feed rate. For the AA4XXX-T6, however, the data scattering showed some minima at specific combinations of speed and feed.

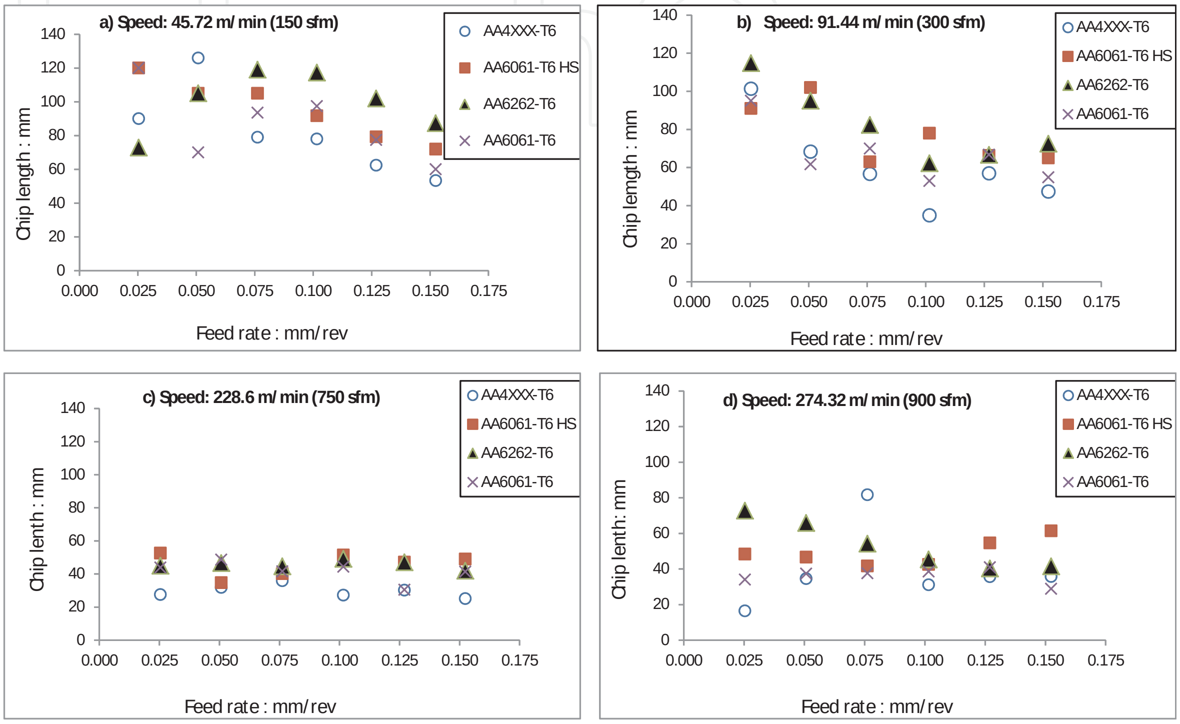

Figure 20. Variation of drilled chip length as a function of feed rate and cutting speeds for the tested alloys

5.6. Partial and global machinability comparisons

In order to compare the performance of the four alloys globally in terms of the various measures of machinability, specific ratios for the main factors of interest were defined. Figure 21 presents a summary of these ratios including, thrust force tendency (Figure 21-a), sticking tendency (Figure 21-b), burr tendency (Figure 21-c) and chip length tendency (Figure 21-d) relative to AA6262-T6.

A higher coefficient value corresponds to a lower machinability. It was observed that AA4XXX-T6 was the worst case, in terms of burr height and thrust force requirement. The latter was probably due to the presence of the high volume faction of second phase consisting of Si particles which also raises the hardness of the AA4XXX-T6. This alloy also had the lowest yield strength and highest elongation which may be related to the poor burr height performance. In contrast, in terms of chip length and sticking tendency the AA4XXX-T6 was equivalent or superior to AA6262-T6. The use of AA6061-T6 HS vs. standard AA6061-T6 gave inferior performance in terms of sticking and chip length which is an interesting result as in often in the industry the trend is to move in this direction to solve machining problems. However, the high strength version was superior in terms of surface roughness and burr height. As expected the AA6262-T6 performed well in most categories but surprisingly in these tests was the worst in terms of chip length.

Figure 22 displays the global machinability of the tested alloys as a function of the weights of the different component of the machinability (λ_1: tool life, λ_2: sticking tendency, $\lambda_{3:}$ cutting force, $\lambda_{4:}$ burr height, $\lambda_{5:}$ chip length and λ_5 surface finish). These weights ($\lambda_{1,}$ $\lambda_{2,}$ $\lambda_{3,}$ λ_4 and $\lambda_{5)}$ must be set according to the application, the machine-tool limitations and the manufacturer preference.

It appears for Figure 22 that amongst the tested alloys, only the AA6061-T6 HS performed better (in spite of its high resistance) that the reference material (AA6262-T6) at all the evaluated combinations. The global performances of the AA6061-T6 and the AA4XXX-T6 are comparable but remains lower that of the AA6262-T6.

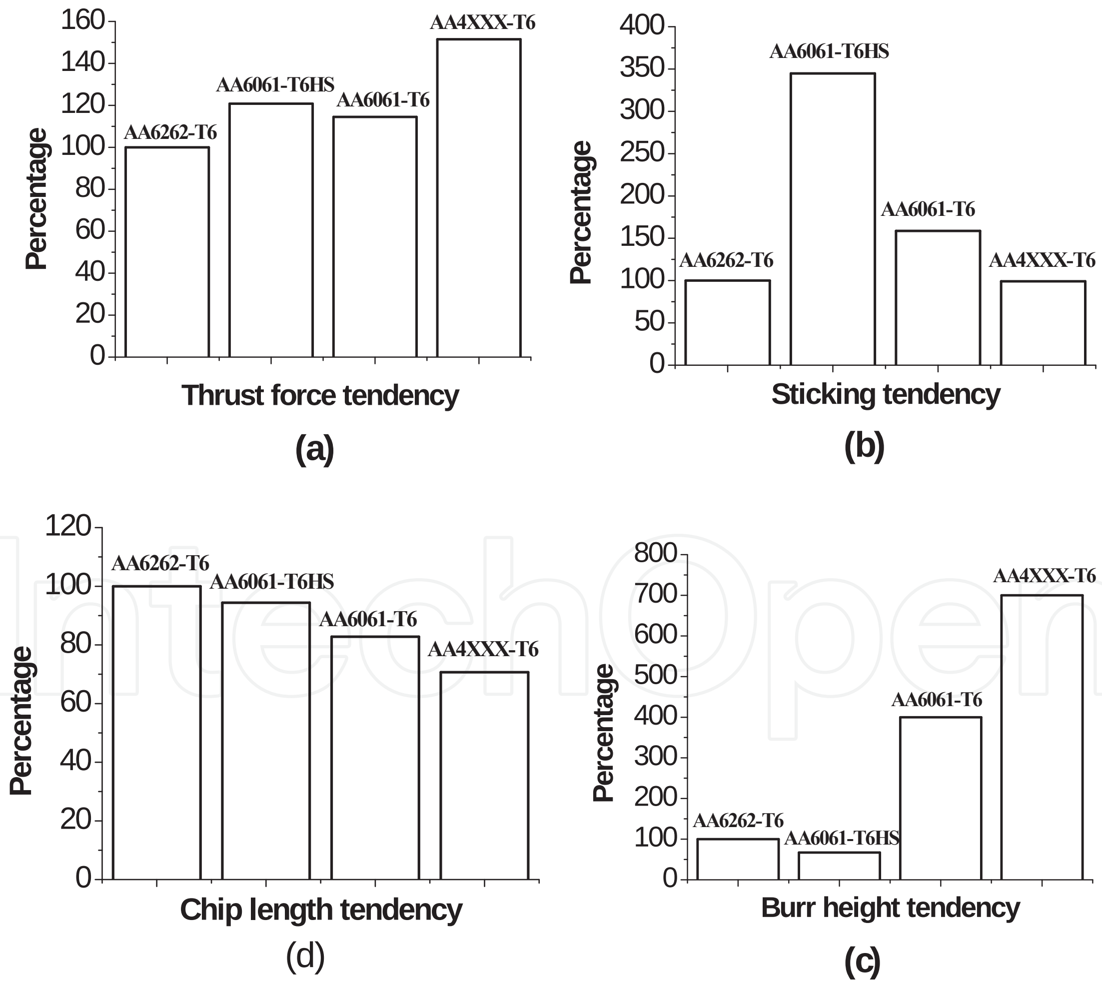

Figure 21. Summary of the force, the sticking, burr and chip length tendency for different tested materials

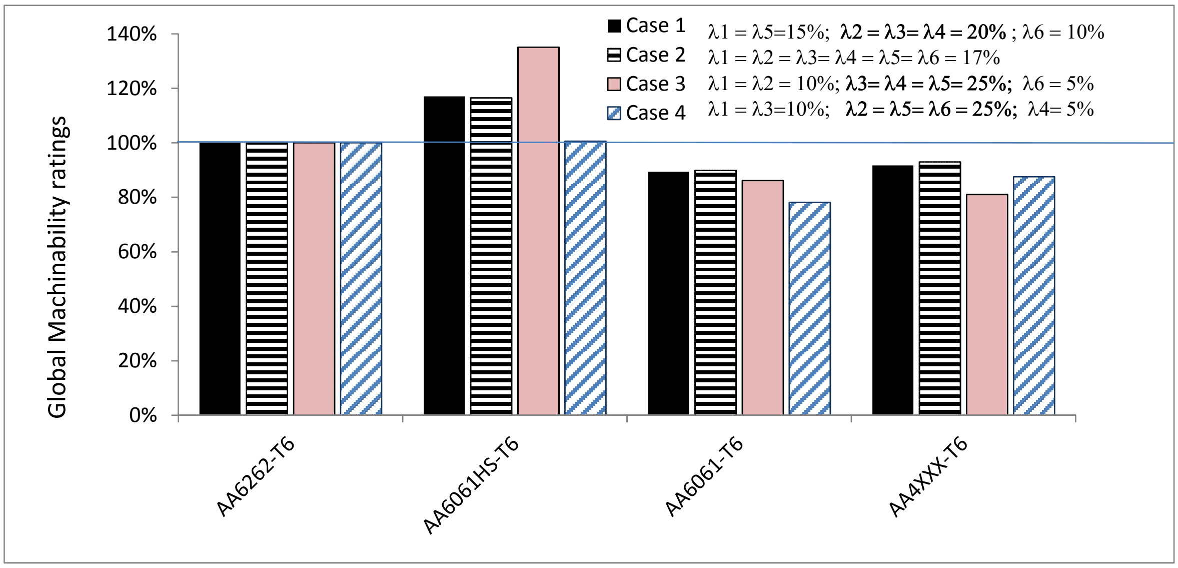

Figure 22. Computed Global Machinability (Eq. 2) for different materials as compared to AA6262-T6

6. Conclusion

The development of aluminum alloys is often conditioned by aeronautical requirements, but aluminum is very interesting for several applications in other sectors. Depending on the nuances, the composition, the treatments and the cutting conditions of these alloys, the material can be classified according to its extrudability, machinability, recyclability, etc. In this work, the machinability performance (tool life, force, surface finish, chip form and burr size) of four commercially available Al-Mg-Si alloys was investigated. It can be concluded that for a non lubricated drilling operation using typical conditions (3/8 inches diameter drill at a cutting speed of 106 m/min (350 sfm)):

- When the global machinability (tool life, material sticking, cutting force, surface finish, chip form and burr size) is concerned, only the AA6061-T6HS) outperformed the benchmark AA6262-T6 while the two other alloys (AA6061-T6 and AA4XXX-T6) showed low machinability compared to the AA6262-T6.
- All the materials exhibited insignificant tool wear after drilling more than 1000 holes. However, when the number of holes reached 1439, the AA6061-T6 HS alloy began to exhibit noticeable wear which may be related to the fact that it had the highest strength compared to others materials. This wear could be reduced by selecting appropriate cutting tool materials or coatings.
- In terms of cutting force, the AA6061-T6HS and the AA6061-T6 were comparable but inferior to the AA6262-T6, whereas the AA4XXX material required the highest force. This may be due to the high volume fraction of Si particles in the microstructure. In a situation

http://dx.doi.org/10.5772/54021

where the machine-tool is powerful enough to accommodate the higher cutting force and the burr could be controlled, the AA4XXX-T6 could become a very interesting material.

- The chip forms obtained were similar for all materials tested: Long or short chips could be obtained depending on the machining conditions. Regardless of the material type, the chip form and the chip management could be controlled by selecting appropriate feeds and speeds.
- In terms of hole quality, the surface finish produced on AA6262-T6 was poor compared to the others alloys tested (AA6061-T6HS, AA6061-T6 and AA-4XXX-T6). The AA6061-T6HS produced a lower burr height which is beneficial in reducing deburring costs.

Author details

V. Songmene[1], J. Kouam[1], I. Zaghbani[1], N. Parson[2] and A. Maltais[2]

1 École de Technologie Supérieure (ÉTS), Montreal, QC, Canada

2 Rio Tinto Alcan, Jonquière, QC, Canada

References

[1] Altintas, Y. (2000), Manufacturing Automation, Cambridge University Press.

[2] Aurich J, Dornfeld D, Arrazola P, Franke V, Leitz L, Min S (2009) Burrs-Analysis, control and removal. CIRP Annals-Manufacturing Technology 58 (2), 519-542

[3] Chena Y., Pedersenb K.O.; Clausena A.H., and O.S. Hopperstada, (2009), An experimental study on the dynamic fracture of extruded AA6xxx and AA7xxx aluminium alloys, Materials Science and Engineering A 523 (2009), 253–262.

[4] Costa E. S., da Silva M. B. and Machado A. R., Burr Produced on the Drilling Process as a Function of Tool Wear and Lubricant-Coolant Conditions, J. of the Braz. Soc. of Mech. Sci. & Eng. Vol. XXXI, No. 1, 2009, 57-63.

[5] Dornfeld, DA., 2004, Strategies for Preventing and Minimizing Burr Formation, Consortium on Deburring and Edge Finishing, (University of California, Berkeley), internal report No Dornfeld-1-04, 19 pages.

[6] Duval, M., (2012), L'Aluminium et sa transformation, notes de cours, ÉTS, Montréal, Canada, 6 juin 2012 (In french).

[7] Farmer, L. E., (1978), a system for evaluating the cold extrudability of Aluminium alloys, Journal of Mechanical Working Technology, 1 (1978), 371-386.

[8] Gillespie, L. K., Deburring and edge finishing, Handbook, 1999.

[9] Gillespie, L.K., 1973, Formation and properties of Machining Burr, M.S. Thesis, Utah State University, Logan, UT.

[10] Hashimura M, Hassamontr J, Dornfeld D (1999) Effect of in-plane exit angle and rake angles on burr height and thickness in face milling operation. Journal of manufacturing science and engineering, 121:13

[11] Kouam J., Masounave J. and Songmene V., (2010) Pre-holes Effect on Cutting Forces and Particle Emission During Dry Drilling Machining, In Proc. of 49th Annual Conf. Metallurgists of CIM, Vancouver, BC, Canada, 2010, 253-263.

[12] Kouam J., Zaghbani I., Songmene V., Parson N. and Maltais A., (2012), Factors affecting the machinability of Al-Mg-Si extrusions, Proc. 10th Int. Aluminum Extrusion Technology Conf., Miami Florida USA, 15-18 May 2012, 443-461.

[13] List G., Nouari M., Ge´hin D., Gomez S., Manaud, J.P. , Le Petitcorps Y. and Girot F., Wear behaviour of cemented carbide tools in dry machining of aluminium alloy, Wear 259 (2005), 1177-1189.

[14] Nouari M., List G., Girot F. and Ge´hin D., Effect of machining parameters and coating on wear mechanisms in dry drilling of aluminium alloys, Machine Tools & Manufacture 45 (2005), 1436-1442.

[15] Niknam, S. A. and Songmene, V., (2012), Modeling of burr thickness in milling of ductile materials, International Journal of Advanced Manufacturing Technology, DOI 10.1007/s00170-012-4479-3

[16] Olvera O., Barrow, G., 1996, An experimental study of burr formation in square shoulder face milling, J. of Mach. Tools Manufacture., vol. 36, No 9, 1005-1020.

[17] Pangborn J.; Hoff E.; Dickson R.; Devadas C., (2012), 6005A: Practical Evidence of Advantages for Extruders and Their Customers, Proc. Tenth international Aluminum Extrusion Technology Seminar & Exposition, May 15-18, 2012, Fontainebleau, Miami Beach Resort, Miami, Florida, USA, 49-54.

[18] Rivero A., Aramendi G., Herranz S. and L´opez de Lacalle L.N., An experimental investigation of the effect of coatings and cutting parameters on the dry drilling performance of aluminum alloys, Advanced Manufacturing Technology (2006) 28, 1-11.

[19] Saha P.K., (2012), Economics of Aluminum Extrusion for Aerospace Applications, Proc. 10th Int. Aluminum Extrusion Technology Conf., Miami Florida USA, 15-18 May 2012, 357-366.

[20] Sandvik C., Modern Metal Cutting - A Practical Handbook, Sweden, 1994.

[21] Shaw M.C., Metal Cutting Principle, Oxford Science, 1989.

[22] Songmene V., Khettabi R., Zaghbani I., Kouam J., and Djebara A., (2011), Machining and Machinability of Aluminum Alloys, Aluminum Alloys, in Theory and Applications", Tibor Kvackaj (Ed.), ISBN: 978-953-307-244-9, InTech, 2011, 377-400.

[23] Songmene V., Stefan, I., Stefan, M., Yan, D., Hirholzer, J., Tool Life & Machinability Testing - Testing Procedure & Database, Report of project, Industrial Research & Development Institute, IRDI, Midland, ON, Canada, Nov. 1996.

[24] Subramanian K. and Cook N.H., Sensing of Drill Wear and Prediction of Drill Life, J. of Engineering for Industry, Trans of ASME, Vol. 99, Series B, 1977, 295-301.

[25] Zaghbani I., Songmene V., A force-temperature model including a constitutive law for Dry High Speed Milling of aluminium alloys, Materials processing technology 209 (2009), 2532-2544.

[26] Zaghbani I., Songmene V., Kientzy G. and Lehuy H., Evaluation of Sustainability of Mould Steels Based on Machinability Data, International Journal Machining and Machinability , Vol. 7, Nos. 1/2, 2010, 58-81.

[27] Zitoune R., Krishnaraj V. and Collombet F., Study of drilling of composite material and aluminium stack, Composite Structures 92 (2010), 1246-1255.

IntechOpen